Published in IET Circuits, Devices & Systems
Received on 13th November 2013
Revised on 23rd January 2014
Accepted on 28th January 2014
doi: 10.1049/iet-cds.2013.0413

Special Issue on Photonic and RF Communications Systems

ISSN 1751-858X

Delay analysis of converged optical-wireless networks with quality of service support

John S. Vardakas[1], Ioannis D. Moscholios[2], Nizar Zorba[3], Michael D. Logothetis[4], Christos V. Verikoukis[5]

[1]Iquadrat, Barcelona, Spain
[2]Department of Informatics and Telecommunications, University of Peloponnese, Tripolis, Greece
[3]Qatar University, Doha, Qatar
[4]WCL, Electrical and Computer Engineering, University of Patras, Patras, Greece
[5]Telecommunications Technological Centre of Catalonia (CTTC), Barcelona, Spain
E-mail: jvardakas@iquadrat.com

Abstract: The convergence of two popular access technologies, namely Worldwide interoperability for Microwave Access (WiMAX) and passive optical network (PON) is a promising access solution that combines the mobility feature of WiMAX and the ample bandwidth of PONs. In such a converged optical-wireless access network, the provision of quality of service (QoS) support is a challenging issue, mainly because of the different bandwidth allocation mechanisms of the two access technologies. Since the considered convergence seems to be dominant, it deserves assiduous analysis and evaluation. In this study, the authors investigate the delay performance of a converged optical-wireless network that provides QoS support by considering multiple service-classes with different priorities. In the wireless domain, the IEEE 802.16 standard is applied, whereas in the optical domain a wavelength division multiplexing ethernet PON provides connectivity to both wired and wireless users. The authors present an analytical framework for the calculation of the average end-to-end packet delay of each service-class, by developing two queuing models for each domain of the converged network. The end-to-end delay is calculated as the sum of the queuing delay in both domains, and the transmission and propagation delay in the optical domain. The accuracy of the proposed analysis has been verified by simulation and found to be quite satisfactory.

1 Introduction

The emergence of bandwidth consuming applications, such as Internet Protocol Television and Video-on-Demand, have boosted the efforts of both service providers and academia to provide efficient and cost-effective access solutions that support differentiated traffic. Indeed, the increasing demand for quadruple play services (broadband, voice, video and mobility) has created new challenges for the development of an access network capable of providing high bandwidth, mobility support and quality of service (QoS) differentiation [1]. The solution can be obtained by the integration of a wireless system and an optical access network, or in other words, by taking advantage of the mobility features of the wireless systems and the bandwidth benefits of fibre-based communications.

A converged optical-wireless access network consists of a wireless sub-network as the front-end and an optical access network as the back-end. Various technologies have been proposed for both sub-networks and have been applied in different converged technologies [2]. Common wireless network designs include Wireless Fidelity (WiFi), Worldwide interoperability for Microwave Access (WiMAX) and Long-Term Evolution (LTE), where the latter two technologies inherently provide QoS support. On the other hand, passive optical networks (PONs) have gained prominence as the back-end optical access technology that is able to provide huge bandwidth in a cost effective manner [3]. A PON is a point-to-multipoint optical network that connects a number of optical network units (ONUs), which are located at the users premises, to an optical line terminal (OLT), which in turn is connected to the core network. Current PON deployments utilise the time division multiplexing (TDM), such as gigabit PON (GPON) and ethernet PON (EPON) that have been deployed in USA, Europe and Japan [4]. A promising solution for upgrading an EPON is the adoption of the wavelength division multiplexing (WDM) technology. The resulting wavelength division multiplexing ethernet PON (WDM-EPON) is able to provide higher bandwidth to end-users, while supporting services with diverse QoS requirements [5].

In this paper, we focus on the convergence of EPON and WiMAX broadband access networks, whereby the drawback of WiMAX of reducing the data-rate when increasing the distance is drastically faced by the EPON, which can provide 10 Gbps data-rates up to a distance of 20 km [6]. Therefore this optical-wireless network seems to be a

dominant network convergence and deserves assiduous analysis and evaluation. Herein, we present an analytical framework for the calculation of the average packet delay in the uplink of a converged WiMAX and WDM-EPON, capable of providing QoS support. The QoS differentiation is achieved by considering several QoS classes with different service priorities in both the wireless and the optical domain. In the wireless domain the IEEE 802.16 standard is applied, whereas a TDM scheme is considered for the service delivery to different wireless users, because of its ability to offer better service to multiple QoS classes, compared to a frequency division multiplexing scheme [7]. We assume that the converged network supports the four QoS classes that are defined by the IEEE 802.16 standard: the Unsolicited Grant Service (UGS), the real-time Polling Service (rtPS), the non-real-time Polling Service (nrtPS) and the Best Effort (BE) service [8]. In the optical domain, the WDM-EPON provides service to both wired users (through the ONUs) and wireless users (through the base stations (BSs) of the wireless network). The bandwidth allocation to the ONUs is performed by considering the fixed service of the Interleaved Polling with Adaptive Cycle Time (IPACT) protocol [9]. According to the fixed service of the IPACT, the time-slots allocated to each ONU have the same length, as well as the time between two consecutive transmissions is constant. The application of the fixed service simplifies the bandwidth allocation procedure in the EPON, whereas its packet-delay performance under heavy traffic loads is similar to the other IPACT bandwidth allocation services [10]. We assume that each BS in the wireless domain and each ONU in the optical domain transmit batches of packets, within a time-slot duration, which is a rather realistic assumption and in accordance with the two network architecture standards. A time-slot duration is a multiple integer of a time-unit, during which a single packet is transmitted.

For the calculation of the average end-to-end delay in the uplink of the converged network, we derive two analytical models: the first model describes the delay performance in the wireless domain, whereas the second model determines the average packet delay in the optical domain. Under the assumption that packets are served in batches, each analytical model comprises two queuing models: one for the queuing delay in the four queues which correspond to the four QoS classes, and another one for the queuing delay when batches of packets from each QoS class form a frame, according to the IPACT fixed service. We first determine statistics on the batches and then on individual packets. Specifically, we provide the analytical framework for the determination of the mean queue length and the mean waiting time in the batch queuing model. These statistics are then used for the calculation of the average delay of the individual packets. Finally, we determine the total packet delay by adding up the transmission and the propagation delay in the optical domain. The accuracy of the proposed models is verified by simulations and found to be quite satisfactory.

The rest of the paper is organised as follows. In Section 2, we review the related work. In Section 3, we present the system model and the analytical models for the delay calculation in the wireless and optical domain. In Section 4, we evaluate the proposed models by comparing analytical and corresponding simulation results, whereas we study the effect of various parameters to packet delay. We conclude in Section 5.

2 Related work

Several studies of converged optical-wireless networks have been published, regarding architecture and physical layer. The interested reader may resort to [2] for an overview of the research into optical-wireless network architectures. Furthermore, Medium Access Control issues have also been studied. Several bandwidth allocation and scheduling topics are discussed in [11] for various network architectures, such as the independent, the hybrid and the unified connection-oriented architecture. The delay performance of an integrated EPON-WiMAX network is the subject of [12], where authors propose a centralised scheduling mechanism for QoS support. This mechanism has been studied through simulation and proved to provide a better performance in terms of delay and throughput, compared to the Independent Scheduling (IS) mechanism which is used for the transmission scheduling between EPON and WiMAX. Similar studies that evaluate the delay performance of EPON-WiMAX with QoS support through simulation are presented in [13–16], where different scheduling and/or bandwidth allocation schemes are proposed.

To the best of our knowledge, only two publications exist in the literature that propose analytical models for the packet delay calculation in converged EPON-WiMAX networks with QoS support. The model of [17] targets on the queuing delay at the ingress and egress queues of the ONUs, without defining a bandwidth allocation scheme. An analytical model for the calculation of the end-to-end delay in an EPON-WiMAX network is presented in [18]; this model considers multiple service-classes and a bandwidth allocation scheme; however, the model assumes an equal arrival rate of each service-class, whereas it does not consider the different size of packet batches within the transmitted frame.

In summary, in most previous works, the delay performance of a converged WDM-EPON-WiMAX network is studied through simulations, whereas existing analytical models are based on rather simplified assumptions for the packet arrival and transmission processes. We have mathematically analysed the delay performance of the optical domain, only [19]. In this paper, we consider the convergence of WDM-EPON and WiMAX network, and propose an analytical framework for the calculation of end-to-end delay, while considering multiple service-classes and a simple but effective bandwidth allocation scheme. In the proposed model, we assume different packet arrival rates and different number of packets transmitted in each transmission cycle per service-class, for the different BSs and ONUs. Moreover, the proposed delay analysis leads to a parametric model of the number of wavelengths, which is applicable to a back-end either of a WDM-EPON (multiple wavelengths) or EPON (single wavelength). Furthermore, the proposed model can be applied to a variety of converged network topologies that are characterised by diverse traffic demands.

3 System model

We study the converged network of Fig. 1 that supports N ONUs connected to the OLT through a tunable wavelength router. Each ONU provides service to both wired and wireless subscribers. For the provision of wireless services, a number B_n of BS are connected to the ONU n

doi: 10.1049/iet-cds.2013.0413

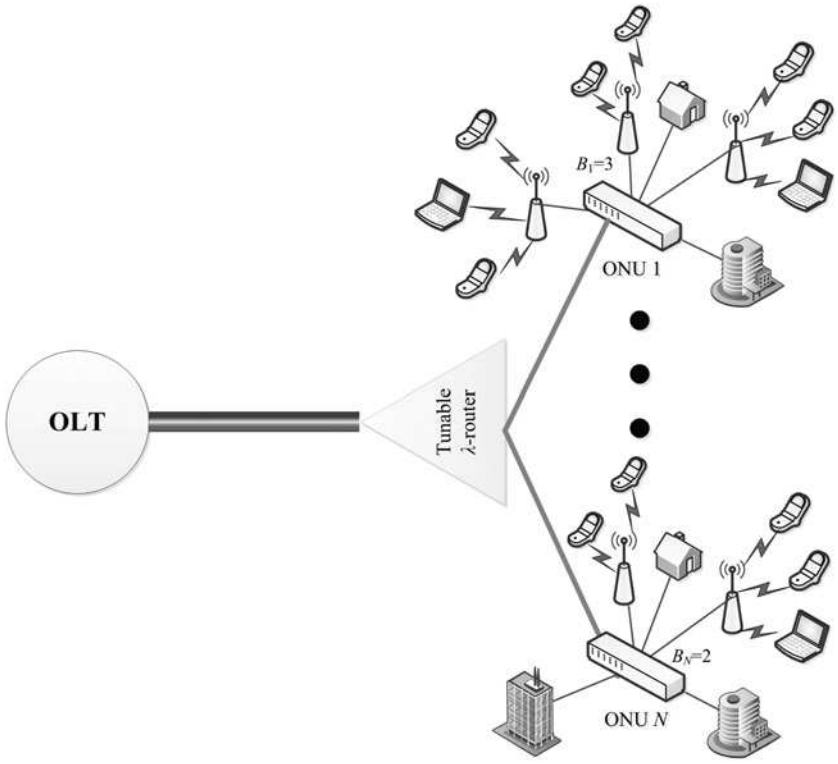

Fig. 1 *A converged optical wireless network*

($n = 1, \ldots, N$) that serve S_{n,b_n} Subscriber Stations (SS), $b_n = 1, \ldots, B_n$. The key feature of the converged network is the provision of different QoS classes that are suitable for data, voice and video services. In the following subsections we provide the system architecture and the analysis in the wireless and optical domains.

3.1 Wireless domain

In the wireless domain, each SS has a number of uplink queues, one for each QoS class. Fig. 2 illustrates a simplified architecture of the SS queues, by considering the four classes of the IEEE 802.16d standard [20]. Packets that belong to QoS-class c ($c = 1$ for UGS, $c = 2$ for rtPS, $c = 3$ for nrtPS and $c = 4$ for BE) wait in the corresponding uplink queue, until they are transmitted to the BS. Each BS is able to transmit batches of packets that form a frame during a specific time interval; this time interval is defined by the characteristics of the uplink queues and the number of SS in the wireless network. We consider that frames of fixed length T_{frame} are allocated to each SS in a non-contention mode; this case is in accordance with the IEEE 802.16d standard. The consideration of fixed length frames results in a fixed time between two consecutive frame transmissions from the same SS to the BS. For simplicity, we consider that the length T_{frame} refers to the

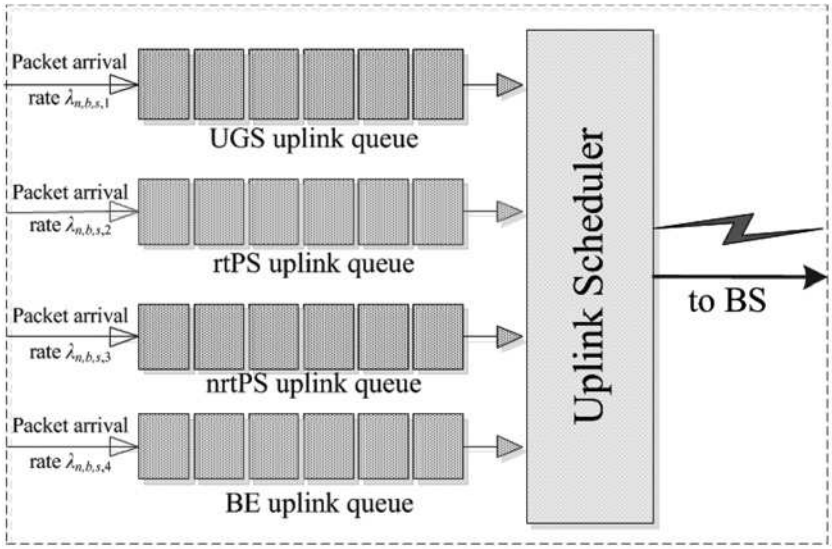

Fig. 2 *Architecture of the SS uplink queues*

uplink packets only, whereas it is equal to

$$T_{\text{frame}} = T_{\text{data}} + T_{\text{hdr}} \tag{1}$$

where T_{data} refers to the data packets of all QoS classes and T_{hdr} to the control packets (preamble, frame control header, uplink map). We also assume that packets transmission takes place during a time-slot of duration σ; all time intervals are measured in time-slots. We also assume that packets of the UGS class have a fixed length of l_1 bits, whereas we assume a variable length for packets of the rtPS, nrtPS and BE classes, with a maximum value of l_2, l_3 and l_4 bits, respectively. The latter assumptions are considered in the IEEE 802.16d standard.

The differentiation between the QoS classes is performed by the allocation of a dissimilar percentage of the frame to each QoS class, so that high-priority classes are able to transmit more packets in each transmission period, compared to low-priority classes. This is achieved by considering the number m_c of time-slots allocated to the QoS-class c so that $m_1 > m_2 > m_3 > m_4$; the latter consideration is applied to all wireless subscribers. As illustrated in Fig. 3, the total number of time-slots that are allocated to all QoS classes is

$$T_{\text{data}} = \sum_{c=1}^{4} m_c \tag{2}$$

The values of m_c are invariable with time and are selected based on the mean queue length of the QoS-class with the highest priority, in order to minimise the packet delay of this class.

We consider that packets of all QoS classes arrive at the corresponding uplink queue according to a Poisson process. Even though the characteristics of independent and identically distributed random arrivals of the Poisson process do not perfectly reflect the packet-level traffic features of wireless networks and PONs, the Poisson process is broadly considered as the starting point of a packet-level teletraffic analysis [21–25]. The arrival rate of the QoS-class c packets in SS $S_{n,bn}$ that is connected to the BS b_n of the ONU n is denoted by $\lambda_{n,b,s,c}$. These packets are served in batches in each frame, where, for each QoS-class, one packet containing the destination address is always transmitted within each batch, together with the data packets. If more than m_c packets wait in the queue, only m_c packets are transmitted, whereas the remaining packets wait for the next transmission frame. The determination of the service time of each queue is based on the time between two consecutive frame transmissions from the same SS. By considering that the BS b_n serves S_{n,b_n} SS, the time interval $T_{n,b}^{\text{w.total}}$ between two consecutive frame transmissions is equal to the sum of the duration of the frames from the remaining $S_{n,b_n} - 1$ SS, plus the sum of the safety intervals δ_w between two consecutive frames

$$T_{n,b}^{\text{w.total}} = \sum_{s=1}^{S_{n,b_n}-1} T_{\text{frame}} \cdot \sigma + (S_{n,b} - 1) \cdot \delta_{\text{w}} \tag{3}$$

The time interval $T_{n,b}^{\text{w.total}}$ is the service time of all queues of all SS that are served by the BS b_n of the ONU n. Equation (3) shows that the service time is constant; therefore, assuming Poisson arrivals, each queue follows an $M/D^{[1,m_c]}/1$ queuing model, with a single server, since a single frame is transmitted in each transmission period. The notation $[1, m_c]$ highlights the transmission of packet batches with a minimum value of 1 (the single packet that contains the destination address) and with a maximum value of m_c packets.

The calculation of the mean queuing delay in the $M/D^{[1,m_c]}/1$ model is based on the formulation of a fictitious M/D/1 queue for the packet batches that are transmitted in each frame. In this fictitious queuing model, the batch service time is constant and equal to $T_{n,b}^{\text{w.total}}$, whereas the number of servers equals 1, since a single batch is transmitted in each transmission period. As far as the batches arrival rate $\lambda_{n,b,s,c}^{\text{w.batch}}$ is concerned, it can be calculated approximately by considering the batch size m_c

$$\lambda_{n,b,s,c}^{\text{w.batch}} = \frac{\lambda_{n,b,s,c}}{m_c} \tag{4}$$

The mean waiting time $W_{n,b,s,c}^{\text{w.batch}}$ of a type-c batch is calculated by considering the mean waiting time in the M/D/1 [26]

$$W_{n,b,s,c}^{\text{w.batch}} = \frac{\lambda_{n,b,s,c}^{\text{w.batch}} \cdot (T_{n,b}^{\text{total}})^2}{2 \cdot \left[1 - \left(\lambda_{n,b,s,c}^{\text{w.batch}} \cdot T_{n,b}^{\text{total}}\right)\right]} \tag{5}$$

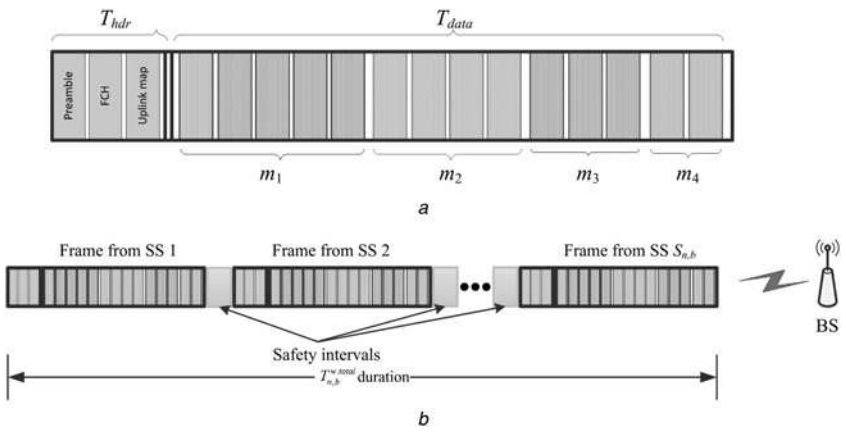

Fig. 3 *Total number of time slots*

a Uplink SS frame to the BS b_n of ONU n

b Determination of the time interval between two consecutive frame transmissions from an SS to the BS

doi: 10.1049/iet-cds.2013.0413

By applying Little's law, we calculate the mean length $L^{\text{w.batch}}_{n,b,s,c}$ of the fictitious M/D/1 queue

$$L^{\text{w.batch}}_{n,b,s,c} = \lambda^{\text{w.batch}}_{n,b,s,c} \cdot W^{\text{w.batch}}_{n,b,s,c} \tag{6}$$

The mean length $L^{\text{w.batch}}_{n,b,s,c}$ of the M/D/1 queue is used to calculate the mean length $L^{\text{w.packet}}_{n,b,s,c}$ of the $M/D^{[1,m_c]}/1$ model, by using the following approximation [27]

$$L^{\text{w.packet}}_{n,b,s,c} \simeq m_c \cdot L^{\text{w.batch}}_{n,b,s,c} + P^{\text{w}}_{n,b,s,c} \cdot \frac{m_c - 1}{2} \tag{7}$$

where $P^{\text{w}}_{n,b,s,c}$ is the probability of waiting in the corresponding fictitious M/D/1 queuing system

$$\begin{aligned} P^{\text{w}}_{n,b,s,c} &= P(j \geq 1) = \sum_{j=1}^{\infty} \pi^{n,b,s,c}_{j} \\ &= 1 - \pi^{n,b,s,c}_{0} = \lambda^{\text{w.batch}}_{n,b,s,c} \cdot T^{\text{w.total}}_{n,b} \end{aligned} \tag{8}$$

where j is the number of batches in the queue. Finally, the mean waiting time of QoS-class c packets is determined by using (8) and applying Little's law

$$W^{\text{w.packet}}_{n,b,s,c} = \frac{L^{\text{w.packet}}_{n,b,s,c}}{\lambda_{n,b,s,c}} \tag{9}$$

3.2 Optical domain

In the optical domain a WDM-EPON is considered, where each ONU is connected to both BS and wired subscribers. We consider that the QoS classes offered to the wireless subscribers are also offered to the wired subscribers. Packets from the wired subscribers are directly forwarded to the corresponding ONU queue, whereas arriving packets from the BS are first extracted from the frames and then forwarded to the ONU queues (Fig. 4). We assume that packets belonging to QoS-class c arrive from the wired subscribers to an ONU following a Poisson process; the arrival rate to ONU n is denoted by $r^{\text{wired}}_{n,c}$. At the same time, batches of QoS-class c packets arrive at the ONU from all the supported BSs of the ONU n, every $T^{\text{w.total}}_{n,b}$ time interval (we assume that the transmission and propagation delay in the wireless domain are negligible, compared to $T^{\text{w.total}}_{n,b}$); therefore, the total number of QoS-class c packets that arrive at ONU n from all B_n BSs in each transmission period equals

$$N_{n,c} = \sum_{b=1}^{B_n} \sum_{s=1}^{S_b} \min\left(m_c, L^{\text{w.packet}}_{n,b,s,c}\right) \tag{10}$$

Note that the number of QoS-class c packets that are transmitted in each transmission period is m_c, if the mean queue length $L^{\text{w.packet}}_{n,b,s,c}$ is higher than m_c, or this number is equal to $L^{\text{w.packet}}_{n,b,s,c}$, when the number of packets in the uplink queues is less than the maximum number m_c. By dividing the number of QoS-class c packets that arrive from each BS by the transmission period $T^{\text{w.total}}_{n,b}$, we derive the average arrival rate of QoS-class c packets from all the SS to the ONU n

$$r^{\text{wireless}}_{n,c} = \left[\sum_{b=1}^{B_n} \sum_{s=1}^{S_b} \min\left(m_c, L^{\text{w.packet}}_{n,b,s,c}\right)\right] \cdot T^{\text{w.total}}_{n,b} \tag{11}$$

By considering both wired and wireless subscribers, the total arrival rate of QoS-class c packets to the ONU n equals

$$R_{n,c} = r^{\text{wired}}_{n,c} + r^{\text{wireless}}_{n,c} \tag{12}$$

The arriving packets are accommodated to the four queues of the ONU in a first-come-first-serve basis. Assuming a Poisson packet arrival process from the wired subscribers and a constant packet inter-arrival time from the wireless subscribers (because of the constant value of $T^{\text{w.total}}_{n,b}$), the resultant arrival process of packets to the ONU queues is approximated as a Poisson process, with a mean arrival rate that is given by (12). This approximation has been widely used in the literature for modelling the superposition of a Poisson and deterministic arrival processes [28, 29].

For the transmission of the received packets to the OLT, the ONUs form frames by following the same procedure, as the one used for the frame formation in the BS. Since the PON supports multiple wavelengths, a number of frames (equal to the number of wavelengths) is transmitted simultaneously by each ONU in each transmission period. We consider that all ONUs support the same number W of wavelengths. In each ONU W transmitters are installed; each transmitter operates on a different wavelength.

The calculation of the mean queuing delay in the ONU queues is realised by following a similar procedure, as the one used for the delay calculation in the SS queues.

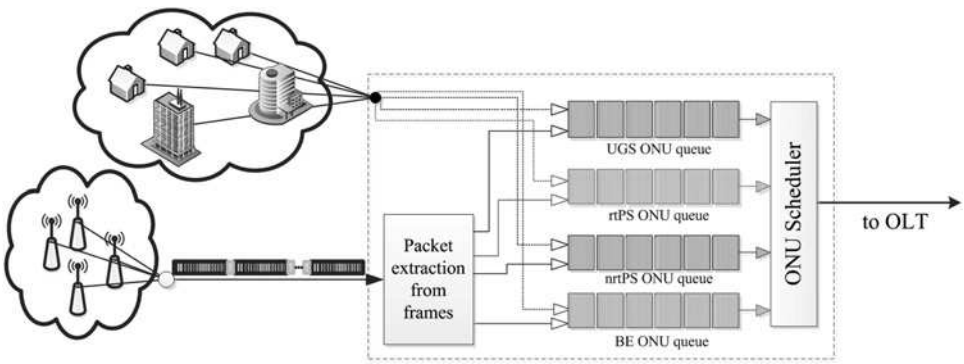

Fig. 4 *Packet arrivals from both wired and wireless subscribers to the ONU*

Specifically, in order to describe the queue for the QoS-class c packets, we consider the $M/D^{[1,d_{n,c}]}/W$ queuing model of W servers, where $d_{n,\,c}$ is the number of QoS-class c packets that are transmitted in each frame. At each transmission period, each transmitter sends a frame to the OLT; thus, W frames per ONU are transmitted simultaneously in each transmission period.

Similar to the same procedure of the previous subsection, we first calculate the time interval between two consecutive frame transmissions from the ONU n. Since the PON supports N ONUs, this time interval equals

$$T_{n,b}^{\text{o.total}} = \sum_{n=1}^{N-1} T_{\text{frame}}^{\text{o}} + (N-1)\cdot\delta_{\text{o}} \tag{13}$$

where $T_{\text{frame}}^{\text{o}} = \sum_{c=1}^{4} d_{n,c}$ is the frame duration and δ_{o} is the safety interval between two consecutive frames. The arrival rate of the type-c batches $R_{n,c}^{\text{o.batch}}$ is a function of the arrival rate $R_{n,c}$ of type-c packets and the batch size $d_{n,c}$

$$R_{n,c}^{\text{o.batch}} = \frac{R_{n,c}}{d_{n,c}} \tag{14}$$

By considering the fictitious queuing system M/D/W for batches, we calculate the mean waiting time of the type-c batches, when using the following approximation, which is derived by the general M/G/W queuing system [27]

$$W_{n,c}^{\text{o.batch}} = \frac{P_{n,c}^{\text{o}}\cdot T_{n,b}^{\text{o.total}}\cdot\sigma}{1-A_{n,c}^{\text{o.batch}}}\cdot\frac{1}{2\cdot W} \tag{15}$$

where $A_{n,c}^{\text{o.batch}} = R_{n,c}^{\text{o.batch}}\cdot T_{n,b}^{\text{o.total}}$, σ is the time-slot duration and $P_{n,c}^{\text{o}}$ is the probability of waiting in the M/D/W system [27]

$$P_{n,c}^{\text{o}} = \frac{\left(W\cdot A_{n,c}^{\text{o.batch}}\right)^{W}}{W!\cdot\left(1-A_{n,c}^{\text{o.batch}}\right)}\cdot\left[\sum_{i=0}^{W-1}\left(\frac{\left(W\cdot A_{n,c}^{\text{o.batch}}\right)^{i}}{i!}\right) + \frac{\left(W\cdot A_{n,c}^{\text{o.batch}}\right)^{W}}{W!\cdot\left(1-A_{n,c}^{\text{o.batch}}\right)}\right] \tag{16}$$

By using the mean waiting time of batches and Little's law, we derive the mean queue length for the batches

$$L_{n,c}^{\text{o.batch}} = R_{n,c}^{\text{o.batch}}\cdot W_{n,c}^{\text{o.batch}} \tag{17}$$

The values of the mean queue length $L_{n,c}^{\text{o.batch}}$ of the fictitious queuing system are used for the calculation of the mean queue length $L_{n,c}^{\text{o.packet}}$ of the individual type-c packets, by applying the following approximation [27]

$$L_{n,c}^{\text{o.packet}} \simeq d_{n,c}\cdot L_{n,c}^{\text{o.batch}} + P_{n,c}^{\text{o}}\cdot\frac{d_{n,c}-1}{2} \tag{18}$$

Finally, the mean waiting time of type-c packets in the corresponding queue is given by Little's law

$$W_{n,c}^{\text{o.packet}} = \frac{L_{n,c}^{\text{o.packet}}}{R_{n,c}} \tag{19}$$

In the wireless domain, packets that are transmitted from end-users to the BS suffer propagation and transmission delay. We assume that the propagation delay is not significant, assuming that end users are close to the BSs [30, 31]. The maximum transmission delay $W_{\text{tr},c}^{\text{w}}$ for QoS class c equals l_c/B^{w}, where l_c is the maximum length of QoS class c packets and B^{w} is the bit-rate in the wireless uplink. Packets that are transmitted from ONUs to the OLT also suffer transmission and propagation delay. Similarly to the transmission delay in the wireless domain, the transmission delay $W_{\text{tr},c}^{\text{o}}$ in the optical domain equals l_c/B^{o}, where B^{o} is the bit-rate in the optical uplink. Furthermore, the propagation delay from ONU n is given by

$$W_{\text{pr}} = \frac{h_n}{\tilde{c}} \tag{20}$$

where h_n is the distance of the ONU n from the OLT, $\tilde{c} = c_0/\tilde{n}$ is the speed of light in the optical fibre, c_0 is the speed of light in the vacuum (3×10^8 m/s) and $\tilde{n}$ is the refractive index of the optical fibre.

By using the aforementioned delay parameters, we calculate the end-to-end packet delay from the SS s that is connected to the BS b_n of the ONU n

$$E[W_c^{\text{wireless}}] = W_{n,b,s,c}^{\text{w.packet}} + W_{n,c}^{\text{o.packet}} + W_{\text{tr}}^{\text{w}} + W_{\text{tr}}^{\text{o}} + W_{\text{pr}} \tag{21}$$

whereas, for the wired subscribers, the mean end-to-end delay is

$$E[W_c^{\text{wired}}] = W_{n,c}^{\text{o.packet}} + W_{\text{tr}} + W_{\text{pr}} \tag{22}$$

4 Evaluation and discussion

We evaluate the proposed analysis through simulation. To this end, we consider a WDM-EPON-WiMAX network that supports $N = 16$ ONUs and tackle two evaluation scenarios. For presentation purposes, in the first scenario each ONU supports 10 BS ($B_n = 10$), whereas each BS provides service to the same number $S_{n,b} = 50$ of end-users. In the wireless domain, the frame duration is $T_{\text{frame}} = 1$ ms, whereas the time-slot duration is $\sigma_{\text{w}} = 50$ µs, and the safety interval is $\delta_{\text{w}} = 50$ µs. The number of packets from each class that are transmitted in each frame is $m_1 = 10$, $m_2 = 7$, $m_3 = 5$ and $m_4 = 3$, per BS and ONU, (in accordance to (2)). In order to highlight the delay differentiation among the QoS classes because of the frame distribution, we assume that users of all QoS classes transmit packets of the same length, which is equal to 1500 bytes, whereas the transmission rate is assume to be equal to 25 Mbps. Furthermore, we assume an error free channel, whereas the propagation in the wireless domain is negligible, compared to the queuing delay. In the optical domain, the values of the applied parameters are listed in Table 1.

For this evaluation, a simulator has been built by using Simscript III [32]. All simulation results have been obtained with ten replications, each time with a different random seed, and 95% confidence interval. The simulator is based on the network model presented in the previous section and considers the set of SS uplink queues and the set of the queues in each ONU. A number of 2×10^6 packets are transmitted from both wired and wireless users, whereas the

doi: 10.1049/iet-cds.2013.0413

Table 1 Values of the parameters used in the optical domain of the first application scenario

Parameter	Value
number of wavelengths W	4
distance h_n	10 km
frame T^o_{frame}	10 ms
safety interval δ_o	50 μs
slot duration σ	50 μs
($d_{n,1}$, $d_{n,2}$, $d_{n,3}$, $d_{n,4}$)	(80, 60, 40, 20) packets
packet length l	1000 bits
upstream channel bit-rate B	1 Gbps
refractive index $\tilde{n}$	1.45

simulation metrics are saved after the service of the first 2×10^5 packets, in order to ensure that the metrics are obtained when the system is in steady state. The arrival procedure is configured in the simulation setup as a Poisson process, whereas an error-free channel is assumed for the wireless users.

We first study the impact of the packet arrival rate to the end-to-end delay. In Table 2, we present analytical and simulation results for the average end-to-end delay of the BE and nrtPS QoS classes, against the packet arrival rate. Similarly, in Table 3 we present analytical and simulation results for the average end-to-end delay of the rtPS and UGS QoS classes. We consider an equal mean arrival rate for all QoS-classes, in order to have a common benchmark for the end-to-end delay. As the results reveal, the accuracy of the proposed models is quite satisfactory; because of the approximations of (7) and (18), the proposed analytical framework overestimates the queuing delay and therefore analytical results are slightly higher than the corresponding simulation results. Furthermore, as it was anticipated, the high priority QoS classes perform better in terms of the end-to-end delay.

In the first application scenario, we study the effect of the frame size distribution on the QoS classes in both optical and wireless domains. We assume a constant frame size $T^{\text{o}}_{\text{frame}}$, whereas we alter the frame distribution to the QoS classes, only in the optical domain, as indicated in the first four columns of Table 4. The arrival rates of the four service-classes are also kept constant; for both the wired and the wireless users the arrival rate is 28 packets/s. In Table 4, we present analytical results for the end-to-end delay of the four QoS classes, together with the delay only in the optical domain; the latter results are presented since the frame distribution is altered only in the optical domain. We observe that the increase of the batch size of the two higher-priority QoS classes reduces their packet delay, especially in the optical domain. This reduction has a negative effect on the delay of the two lower-priority service-classes. This behaviour is because of the frame distribution to the QoS classes, as indicated in the first four columns of Table 4. When the number of high-priority packets in the frame increases, the number of low-priority packets in the transmitting frame reduces; therefore more high priority packets are transmitted in each transmitting period, which results in low delay for these packets. In contrast, the small number of the transmitted low-priority packets results in the increase of the delay of low-priority classes.

In the first application scenario we also study the effect of the number of wavelengths and the number of ONUs on the end-to-end delay. The number of wavelengths equals the number of frames that are simultaneously transmitted by

Table 2 Analytical and simulation results for the end-to-end packet delay of BE and nrtPS QoS classes, in the first application scenario.

Arrival rate	BE delay, ms		nrtPS delay, ms	
(packets/s)	Analysis	Simulation	Analysis	Simulation
20	48.36	47.19 ± 0.732	37.65	36.36 ± 0.535
21	50.94	49.70 ± 0.819	38.46	37.15 ± 0.599
22	53.72	52.42 ± 0.874	39.32	37.97 ± 0.626
23	56.74	55.37 ± 0.932	40.20	38.83 ± 0.655
24	60.02	58.57 ± 0.970	41.13	39.72 ± 0.658
25	63.59	62.05 ± 1.032	42.09	40.65 ± 0.703
26	67.48	65.84 ± 1.145	43.10	41.63 ± 0.724
27	71.73	69.99 ± 1.218	44.16	42.64 ± 0.770
28	76.39	74.53 ± 1.250	45.26	43.71 ± 0.785
29	81.51	79.54 ± 1.274	46.41	44.82 ± 0.793
30	87.19	85.08 ± 1.379	47.61	45.98 ± 0.806

Table 3 Analytical and simulation results for the end-to-end packet delay of the rtPS and UGS QoS classes. in the first application scenario

Arrival rate	rtPS delay, ms		UGS delay, ms	
(packets/s)	Analysis	Simulation	Analysis	Simulation
20	35.36	34.15 ± 0.476	31.01	29.95 ± 0.388
21	35.82	34.59 ± 0.477	31.29	30.22 ± 0.395
22	36.29	35.05 ± 0.482	31.57	30.49 ± 0.398
23	36.78	35.52 ± 0.481	31.86	30.77 ± 0.404
24	37.28	36.00 ± 0.493	32.15	31.05 ± 0.411
25	37.79	36.50 ± 0.503	32.45	31.34 ± 0.417
26	38.32	37.01 ± 0.511	32.76	31.63 ± 0.433
27	38.87	37.53 ± 0.545	33.06	31.93 ± 0.444
28	39.42	38.07 ± 0.559	33.38	32.24 ± 0.459
29	40.00	38.63 ± 0.575	33.70	32.55 ± 0.458
30	40.59	39.20 ± 0.589	34.03	32.86 ± 0.472

Table 4 End-to-end delay and delay in the optical domain results for various frame distributions

Frame distribution				End-to-end delay (delay in the optical domain), ms			
$d_{n,1}$	$d_{n,2}$	$d_{n,3}$	$d_{n,4}$	BE	nrtPS	rtPS	UGS
35	25	25	15	33.46 (0.238)	39.70 (0.683)	44.74 (0.774)	72.97 (4.213)
36	26	24	14	33.43 (0.214)	39.61 (0.593)	44.79 (0.824)	73.25 (4.491)
37	27	23	13	33.42 (0.204)	39.57 (0.559)	44.93 (0.958)	74.29 (5.530)
38	28	22	12	33.40 (0.185)	39.51 (0.490)	44.99 (1.023)	74.62 (5.855)
39	29	21	11	33.40 (0.177)	39.48 (0.463)	45.17 (1.203)	76.06 (7.304)
40	30	20	10	33.38 (0.161)	39.42 (0.409)	45.26 (1.289)	76.39 (7.626)
41	31	19	9	33.37 (0.154)	39.40 (0.388)	45.50 (1.537)	78.38 (9.618)
42	32	18	8	33.36 (0.140)	39.36 (0.345)	45.62 (1.653)	78.62 (9.855)
43	33	17	7	33.35 (0.135)	39.34 (0.328)	45.97 (2.002)	81.50 (12.743)
44	34	16	6	33.34 (0.124)	39.31 (0.293)	46.13 (2.160)	82.63 (13.875)
45	35	15	5	33.34 (0.119)	39.30 (0.280)	46.63 (2.663)	95.42 (26.657)

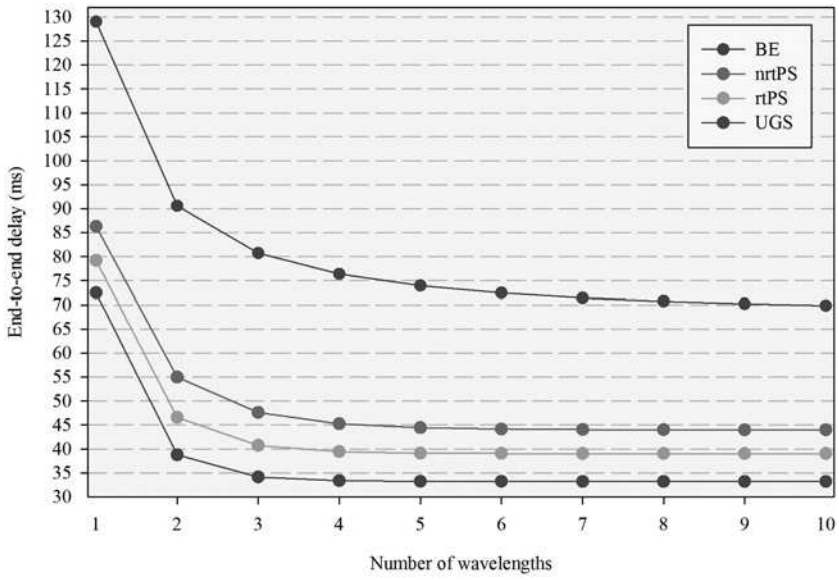

Fig. 5 *End-to-end analytical results against the number of supported wavelengths*

each ONU, in each transmission cycle; therefore, according to Fig. 5, the increase of the number of wavelengths results in the delay decrease for all QoS classes, since more frames are simultaneously transmitted, and more packets of all QoS classes are conveyed in each transmitting period. The results of Fig. 5 are obtained for wireless users, while considering that the arrival rate is the same for all end-users and equals 28 packets/s. Note that the end-to-end delay values, that is the sum of the queuing and transmission delay values in the wireless domain, plus the transmission and propagation delay values in the optical domain, converge to (33.20, 38.94, 43.96, 67.78) ms, which are not affected by the number of wavelengths; this is clearly shown in Fig. 5. Furthermore, in Fig. 6 we present analytical results for the end-to-end delay of all QoS classes against the number of ONUs. The results of Fig. 6 are obtained by using the same parameter set of Fig. 5, when $W = 4$. The increase of the ONU number results in the increase of the number of transmitting users and therefore in the increase of the packet arrival rate. As a result, under high packet arrival-rate conditions, more packets arrive at the ONU queues and need to wait more time for service. Consequently, the proposed model can be used for the derivation of the optimal parameter set, which ensures that the end-to-end delay is kept below predefined levels.

Finally, the second application scenario highlights the effect of the different arrival rate distributions (among the ONUs), on the delay of wired and wireless users. To this end, we consider the same parameter set, as the one used in the first scenario, but the arrival rates of different ONUs and BSs are as listed in Table 5. By applying this arrival rate set on the proposed model, we obtain different delay results for BS and each ONU; therefore, in Table 5 we present the minimum and maximum end-to-end delay of each QoS class. The results of Table 5 reveal that the delay statistics are strongly affected by the arrival-rate values.

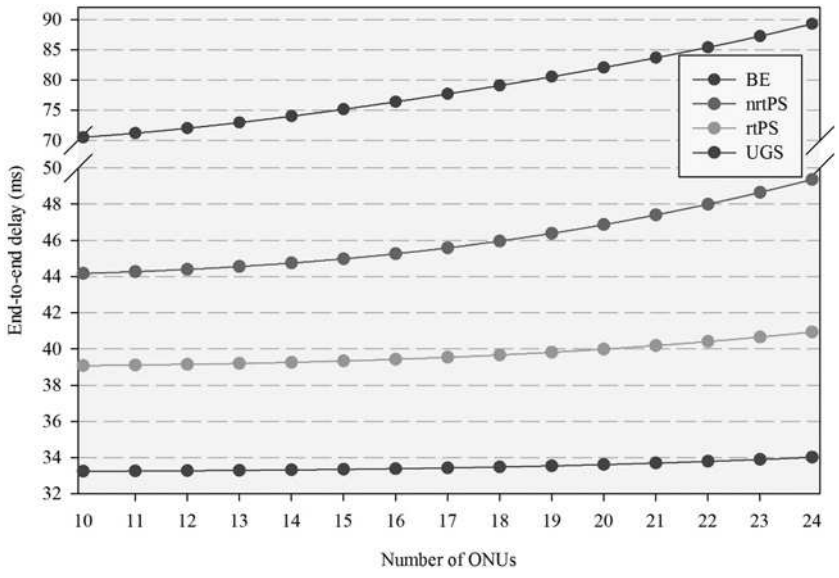

Fig. 6 *End-to-end analytical results against the number of supported ONUs*

doi: 10.1049/iet-cds.2013.0413

Table 5 Analytical results for the end-to-end delay for wired and wireless users, under various arrival-rate distributions

	Arrival rate distribution (packets/s)		End-to-end delay, ms	
	$(\lambda_{n,\ b,\ s,1}, \lambda_{n,\ b,\ s,2}, \lambda_{n,\ b,\ s,3}, \lambda_{n,\ b,\ s,4})$	$\left(r_{n,1}^{\text{wired}}, r_{n,2}^{\text{wired}}, r_{n,3}^{\text{wired}}, r_{n,4}^{\text{wired}}\right)$	Wired users	Wireless users
$n = 2,4,\ldots,16$	(20, 18, 16, 14)	(25, 23, 21, 19)	(30.1, 33.5, 33.6, 34.7)	(31.4, 35.2, 36.2, 41.8)
$n = 1,3,\ldots,15$	(22, 19, 17, 15)	(27, 25, 23, 21)	(30.6, 33.9, 34.3, 36.1)	(32.1, 35.8, 37.3, 44.6)
$n = 2,4,\ldots,16$	(22, 20, 18, 16)	(28, 26, 24, 22)	(30.7, 34.4, 34.9, 37.6)	(32.2, 36.4, 38.3, 47.1)
$n = 1,3,\ldots,15$	(24, 21, 19, 17)	(29, 27, 25, 23)	(31.0, 34.8, 35.6, 39.2)	(32.7, 36.9, 39.3, 49.7)
$n = 2,4,\ldots,16$	(24, 22, 20, 18)	(30, 28, 26, 24)	(31.2, 35.3, 36.4, 40.9)	(32.8, 37.5, 40.4, 52.4)
$n = 1,3,\ldots,15$	(26, 23, 21, 19)	(31, 29, 27, 25)	(31.8, 35.7, 37.1, 42.8)	(33.5, 38.2, 41.5, 55.3)
$n = 2,4,\ldots,16$	(26, 24, 22, 20)	(32, 30, 28, 26)	(31.8, 36.2, 37.9, 44.7)	(33.6, 38.8, 42.7, 58.3)
$n = 1,3,\ldots,15$	(28, 25, 23, 21)	(33, 31, 29, 27)	(32.2, 36.7, 38.7, 46.9)	(34.3, 39.5, 43.9, 61.5)
$n = 2,4,\ldots,16$	(28, 26, 24, 22)	(34, 32, 30, 28)	(32.3, 37.2, 39.5, 49.1)	(34.7, 40.2, 45.2, 64.8)
$n = 1,3,\ldots,15$	(30, 27, 25, 23)	(35, 33 ,31 ,29)	(33.0, 37.7, 40.4, 51.6)	(35.1, 40.9, 46.5, 68.4)
$n = 2,4,\ldots,16$	(30, 28, 26, 24)	(36, 34 ,32 ,30)	(33.1, 38.2, 41.3, 54.3)	(35.4, 41.6, 47.9, 72.3)
$n = 1,3,\ldots,15$	(32, 29, 27, 25)	(37, 35, 33, 31)	(33.6, 38.7, 42.2, 57.3)	(36.0, 42.4, 49.4, 76.5)
$n = 2,4,\ldots,16$	(32, 30, 28, 26)	(38, 36, 34, 32)	(33.7, 39.3, 43.1, 60.5)	(36.2, 43.2, 50.9, 81.2)
$n = 1,3,\ldots,15$	(34, 31, 29, 27)	(39, 37, 35, 33)	(34.3, 40.4, 45.2, 67.9)	(36.9, 44.7, 53.8, 92.1)

5 Conclusion

We present an analytical framework for the determination of the end-to-end delay in a converged WDM-EPON-WiMAX network that supports QoS differentiation. The proposed model assumes that packets belong to multiple QoS classes with different priorities. This prioritisation is expressed by the allocation of a dissimilar percentage of the frame duration to each QoS class. The consideration of the transmission of batches in each transmission cycle leads to the development of two queuing models in both the wireless and optical domain; the first queuing model refers to the batches, whereas the second model refers to the individual packets. Based on these models, we calculate the average end-to-end delay as the sum of the queuing delay in both domains, and the transmission and propagation delay in the optical domain. The accuracy of the proposed calculations is quite satisfactory as was verified by simulations. The proposed model can be used by the network operator to determine the optimal set of network parameters, such as the number of the supported wavelengths or the distribution of packets in the transmitted frames. In this way, the converged WDM-EPON-WiMAX network is capable of the provision of QoS guarantees to the end users, in terms of low packet delays. In our future work, we will consider two different cases for the wireless domain: the first case refers to the IEEE 802.16d, where users are able to transmit multiple packets in the same time-slot by considering multiple sub-carriers, and the second case is the use of the LTE. Moreover, we intend to determine the packet delay distribution, which is the first step for the determination of higher moments of the packet delay.

6 Acknowledgment

This work has been funded by the Research Project COMANDER (EU-Grant: 612257).

7 References

1 Fadlullah, Z., Nishiyama, H., Kato, N., Ujikawa, H., Suzuki, K., Yoshimoto, N.: 'Smart FiWi networks: challenges and solutions for QoS and green communications', *IEEE Intell. Syst.*, 2013, **28**, (2), pp. 86–91

2 Kazovsky, L., Wong, S.W., Ayhan, T., Albeyoglu, K.M., Ribeiro, M.R., Shastri, A.: 'Hybrid optical-wireless access networks', *Proc. IEEE*, 2012, **100**, (5), pp. 1197–1225

3 Srivastava, A.: 'Next generation PON evolution', Proc. SPIE – Int. Soc. Opt. Eng. 8645, 2013, pp. 864509-1–864509-15

4 Grobe, K., Elbers, J.-P.: 'PON in adolescence: from TDMA to WDM-PON', *IEEE Commun. Mag.*, 2008, **46**, (1), pp. 26–34

5 Ansari, N., Jingjing, Z.: 'Media access control and resource allocation in WDM PON', in Ansari, N., Jingjing, Z. (Eds.): 'Media access control and resource allocation' (Springer, 2013), pp. 53–65

6 Madamopoulos, N., Peiris, S., Antoniades, N., Richards, D., Pathak, B., Ellinas, G., Dorsinville, R., Ali, M.A.: 'A fully distributed 10G-EPON-based converged fixed-mobile networking transport infrastructure for next generation broadband access', *IEEE/OSA J. Opt. Commun. Netw.*, 2012, **4**, (5), pp. 366–377

7 Li, B., Qin, Y., Low, C.P., Gwee, C.L.: 'A survey on mobile WiMAX', *IEEE Commun. Mag.*, 2007, **45**, (12), pp. 70–75

8 Papapanagiotou, I., Toumpakaris, D., Lee, J., Devetsikiotis, M.: 'A survey on next generation mobile WiMAX networks: objectives, features and technical challenges', *IEEE. Commun. Surv. Tutor.*, 2009, **11**, (4), pp. 3–18

9 Kramer, G., Mukherjee, B., Pesavento, G.: 'Interleaved polling with adaptive cycle time (IPACT): A dynamic bandwidth distribution scheme in an optical access network', *Photonic Netw. Commun.*, 2002, **4**, (1), pp. 89–107

10 Kramer, G., Mukherjee, B., Pesavento, G.: 'IPACT: a dynamic protocol for an Ethernet PON (EPON)', *IEEE Commun. Mag.*, 2002, **40**, (2), pp. 74–80

11 Shen, G., Tucker, R., Chae, C.-J.: 'Fixed mobile convergence architectures for broadband access: Integration of EPON and WiMAX', *IEEE Commun. Mag.*, 2007, **45**, (8), pp. 44–50

12 Jung, B., Choi, J., Han, Y., Kim, M., Kang, M.: 'Centralized scheduling mechanism for enhanced end-to-end delay and QoS support in integrated architecture of EPON and WiMAX', *J. Lightwave Technol.*, 2010, **28**, (16), pp. 2277–2288

13 Tang, T., Shou, G., Hu, Y., Guo, Z.: 'Performance analysis of bandwidth allocation of convergence of WiMAX and EPON'. Proc. IEEE NSWCTC '09, Wuhan, China, 25–26 April 2009

14 Maier, M., Ghazisaidi, N.: 'QoS provisioning techniques for future fiber-wireless (FiWi) access networks', *Future Internet*, 2010, **2**, (2), pp. 126–155

15 Yang, K., Ou, S., Guild, K., Chen, H.: 'Convergence of ethernet PON and IEEE 802.16 broadband access networks and its QoS-aware dynamic bandwidth allocation scheme', *IEEE J. Sel. Areas Commun.*, 2009, **27**, (2), pp. 101–116

16 Lin, H.-T., Lai, C.-L., Huang, Y.-C.: 'Dynamic bandwidth allocation with QoS support for integrated EPON/WiMAX networks'. Proc. 14th IEEE HPSR, Vancouver, Canada, 8–11 July 2013, pp. 74–79

17 Obele, B.O., Iftikhar, M., Manipornsut, S., Kang, M.: 'Analysis of the behavior of self-similar traffic in a QoS-aware architecture for integrating WiMAX and GEPON', *J. Opt. Commun. Netw.*, 2009, **1**, (4), pp. 259–273

18 Dhaini, A., Ho, P., Jiang, X.: 'QoS control for guaranteed service bundles over fiber-wireless (FiWi) broadband access networks', *J. Lightwave Technol.*, 2011, **29**, (10), pp. 1500–1513

19 Logothetis, M., Moscholios, I., Boucouvalas, A., Vardakas, J.: 'Delay performance of WDM-EPON for multi-dimensional traffic under the IPACT fixed service and the multipoint control protocol'. Proc. 2nd ETS, Karlskrona, Sweden, 30 September–2 October 2013

20 IEEE 802.16d-2004: 'IEEE standard for local and metropolitan area networks. Part 16: Air interface for fixed broadband wireless access systems', Rev. of IEEE 802.16–2001, 2005

21 Chang, B.J., Chen, Y.L.: 'Adaptive hierarchical polling and Markov decision process based CAC for increasing network reward and reducing average delay in IEEE 802.16 WiMAX networks', *Comput. Commun.*, 2008, **31**, (10), pp. 2280–2292

22 Cerutti, I., Fumagalli, A., Gupta, P.: 'Delay models of single-source single-relay cooperative ARQ protocols in slotted radio networks with Poisson frame arrivals', *IEEE/ACM Trans. Netw.*, 2008, **16**, (2), pp. 371–382

23 Aurzada, F., Scheutzow, M., Herzog, M., Maier, M., Reisslein, M.: 'Delay analysis of Ethernet passive optical networks with gated service', *J. Opt. Netw.*, 2008, **7**, (1), pp. 25–41

24 Ni, C., Gan, C., Chen, H.: 'Joint bandwidth allocation on dedicated and shared wavelengths for QoS support in multi-wavelength optical access network', *IET Commun.*, 2013, **7**, (16), pp. 1863–1870

25 Nowak, D., Murphy, J., Perry, P.: 'Bandwidth allocation in DiffServ-enabled ethernet passive optical networks', *IET Commun.*, 2008, **3**, (3), pp. 391–401

26 Iversen, V.B.: 'Teletraffic engineering and network planning', Department of Photonic Engineering, Technical University of Denmark, 2010

27 Bolch, G., Greiner, S., De Meer, H., Trivedi, K.S.: 'Queueing networks and Markov chains, modeling and performance evaluation with computer science applications' (John Wiley, 2006) pp. 267–269 and 313–314

28 Tachibana, T., Ajima, T., Kasahara, S.: 'Round-robin burst assembly and constant transmission scheduling for optical burst switching networks'. Proc. IEEE Globecom 2003, San Francisco, USA, 1–5 December 2003, vol. 5, pp. 2772–2776

29 McEachen, J.C., Batson, M.S.: 'Modeling cache inconsistencies in an ATM high-speed network interface architecture'. Proc. 42nd IEEE Midwest Symp. Circuits and Systems, Las Cruces, NM, USA, 8–11 August 1999, vol. 2, pp. 813–816

30 Sarkar, S., Yen, H.H., Dixit, S., Mukherjee, B.: 'A novel delay-aware routing algorithm (DARA) for a hybrid wireless-optical broadband access network (WOBAN)', *IEEE Netw.*, 2008, **22**, (3), pp. 20–28

31 Luo, Y., Ansari, N., Wang, T., Cvijetic, M., Nakamura, S.: 'A QoS architecture of integrating GEPON and WiMAX in the access network'. Proc. IEEE Sarnoff Symp., Princeton, NJ, USA, 27–28 March 2006

32 Simscript III, http://www.simscript.com/

doi: 10.1049/iet-cds.2013.0413